Radiation Measurements 46 (2011) 2086–2089

Contents lists available at ScienceDirect

Radiation Measurements

journal homepage: www.elsevier.com/locate/radmeas

Measurement of some dosimetric parameters for two mammography systems using thermoluminescent dosimetry

Raúl E. Camargo-Mendoza [a], Martin E. Poletti [a,*], Alessandro M. Costa [a], Linda V.E. Caldas [b]

[a] Departamento de Física, FFCLRP, Universidade de São Paulo, Ribeirão Preto 14040-901, São Paulo, Brazil

[b] Instituto de Pesquisas Energéticas e Nucleares, Comissão Nacional de Energia Nuclear, São Paulo, SP, Brazil

Keywords:
Backscatter factor
Dosimetry
Mammography

ABSTRACT

The Backscatter Factors (BSF), Entrance-Surface Dose (ESD) and Relative Depth Dose (RDD) were assessed by Thermoluminescent Dosimetry (TLD) technique. The measurements have been made varying the geometric and spectral conditions, corresponding to the most radiographic techniques employed in conventional and computer mammographic procedures, i.e., beam qualities in the range of 0.35–0.43 mmAl, tube voltages from 25 kV to 32 kV, anode/filter combinations (Mo/Mo, Mo/Rh and Rh/Rh), different focus-image detector distances from 56 cm to 66 cm, area of irradiation (81, 157, 234 and 432 cm^2) and thickness of the phantom. Results indicate that BSF values show a slight dependence on the various parameters considered, except with the variation of the focus-film distance, where found that this parameter does not have influence on the BSF. ESD values show a strong dependence on the various parameters considered, showing substantially lower values (40%) for computer mammography. RDD curves decrease nearly exponentially with the depth and depend strongly on the spectral conditions. The obtained values show a satisfactory agreement with other studies obtained through Monte Carlo simulation, ionization chambers and thermoluminescent dosimeters.

1. Introduction

Mammography is at present the most effective means of detecting early-stage breast cancer. Over the past 30 years many significant technologic improvements have been made in mammographic equipment in order to produce an image with high contrast, high spatial resolution, and with minimal radiation dose possible. Two dosimetric quantities are important in mammography: Entrance-Surface Dose (ESD) and Relative Depth Dose (RDD) (Stanton et al., 1984; Dance, 1990; Zoetelief et al., 1996). The former involves a measurement in air under scatter-free conditions (incident air kerma) and the application of a backscatter factor (BSF), while the latter is obtained from the knowledge of the relationship between Entrance-Surface Dose and absorbed dose to tissue at depth.

Such factors have been measured by some authors (Dubuque et al., 1977; Hammerstein et al., 1979; Stanton et al., 1981, 1982, 1984; Klevenhagen, 1989; Harrison et al., 1990; Aznar et al., 2005) and have been calculated by others using Monte Carlo techniques (Chan and Doi, 1981; Grosswendt, 1984, 1990; Dance, 1990; Dance et al., 1999; Kramer et al., 2001; Cunha et al., 2010) for conventional and digital mammography. It is important to mention that most of these studies were performed in calibration laboratories, or developed using computational calculations (Monte Carlo) in geometric and spectral conditions slightly different from those found in the current mammograms. Thus the experimental determination of these quantities using clinical mammographic equipment can be more appropriate nevertheless more complex. On the other hand, the choice of an appropriate dosimeter is also a mandatory factor, because it can contain significant systematic errors due to the energy response and the size and location of the dosimeter used. Therefore, small and tissue-equivalent dosimeters are preferable because they will not significantly perturb the radiation field.

In this work, we used Thermoluminescent Dosimetry (TLD) technique to investigate the dependencies of the BSF, ESD and RDD on the geometric and spectral conditions, corresponding to the most radiographic techniques employed in conventional and computer mammographic procedures, i.e., beam qualities in the range of 0.35–0.43 mmAl, tube voltages from 25 kV to 32 kV, focus-image detector distances from 56 cm to 66 cm, area of irradiation (81, 157, 234 and 432 cm^2) and thickness of the phantom from 2 cm to 8 cm. Our results were compared with those previously published obtained through Monte Carlo simulation, ionization chambers and thermoluminescent (TL) dosimeters.

* Corresponding author.
E-mail address: poletti@ffclrp.usp.br (M.E. Poletti).

1350-4487/$ – see front matter © 2011 Elsevier Ltd. All rights reserved.
doi:10.1016/j.radmeas.2011.06.019

2. Materials and methods

2.1. Experimental equipments

Two types of mammographic equipments were used in this study. The first was a Senographe DMR (GE Medical System). This unit allows selecting several anode/filter combinations, as Mo/Mo, Mo/Rh and Rh/Rh. The second equipment was a Mammomat 3000 (Siemens). The possible anode/filter combinations for this unit are Mo/Mo and Mo/Rh.

A total of 42 TL dosimeters was used. The thermoluminescent dosimeters are LiF: Mg, Ti (TLD-100) in the form of extruded square ribbons (about $3 \times 3 \times 0.9$ mm^3) manufactured by Harshaw. TLD-100 was used in this work since it offers an atomic number close to the tissue and small size, characteristics advantageous for this type of measurements. Thermoluminescent readouts were performed using Harshaw Model 2000 TL analyzer. The system consists of two components: the Model 2000-B automatic integrating picoammeter and the Model 2000-C TL detector set to a heating rate of 8 °C/s, with nitrogen flow to suppress chemiluminescence. Readouts were recorded over the 25 s interval between 50 and 250 °C. An oven and a furnace were used for annealing the LiF: Mg, Ti dosimeters. The annealing procedure used consists of two subsequent annealings: 1 h at 400 °C and 2 h at 100 °C. The TL dosimeters were irradiated within two days after annealing. The batch of 42 TL dosimeters used in the experiments was irradiated uniformly with a ^{137}Cs reference source (662 keV) and a calibration coefficient derived for each detector. The energy dependency of these detectors in the mammography energy range was determined as a function of the beam qualities irradiating these detectors with a reference mammographic X-ray tube (Tomal et al., 2010).

The breast is simulated by a polymethylmethacrylate (PMMA) phantom, comprising of semicircular slabs of thickness 10 mm and 100 mm of radius. For RDD measurements small cavities were machine in the upper surface of each semicircular slab for the insertion of dosimeters. Square PMMA slabs (30×30 cm) with thickness of 10 mm were used for studying the variation of BSF with the irradiated area of the phantom.

2.2. Experimental procedure

The determination of the backscatter factors were done through the ratio of the radiation dose at a point on the surface of the phantom (surface measurement condition or ESD) to that at the same point in the absence of the phantom (air measurement condition). The ESD was determined by the net TL readout multiplied by the calibration coefficient and corrected by an energy dependence factor, in this case the TL detector was placed on the surface of the phantom in order to determine the total energy absorbed from both the incident primary beam and the backscattered photons coming out the phantom. For the determination of the absorbed energy due to incident primary (air measurement condition) a special support was constructed in order to place the TL detectors at the same location without the phantom. The support contained four thin plastic wires normally used for fishing stretched across its front surface to hold the TL detectors. These materials did not present any significant attenuation of the X-ray beam or contribute to the scattered radiation. Each surface and air measurement consisted of the simultaneous irradiation of three TL detectors and was repeated three times. The RDD was determined by the ratio of the absorbed dose at depth to ESD. The absorbed dose at depth i (=1 cm, 2 cm, 3 cm,...) was determined by the net TL readout multiplied by the calibration coefficient and corrected by an energy dependence factor corresponding to the beam quality of each depth, since that the variation of response of the detector with depth (beam quality) needs to be considered (Carlsson and Dance, 1992; Carlsson, 1993). Each absorbed dose at depth consisted of the simultaneous irradiation of three TL detectors and was repeated three times.

During TL detectors exposures an ionization chamber was placed near the edge of the beam to monitor and normalize variations in the beam output.

3. Results and discussion

Fig. 1a shows the results obtained for the values of BSF for different phantom thicknesses and anode-filter combinations at 28 kVp. In Fig. 1b, values of BSF are showed as a function of the irradiated area of the phantom for different tube voltages of the Mo/Mo combination.

Fig. 1a shows that BSF increase with increasing phantom thicknesses (about 1% per centimeter), being lower for the Mo/Mo than for the Rh/Rh combination. Both tendencies are expected once that the scattered component increases when the phantom thickness and the beam energy increase (Cunha et al., 2010). In Fig. 1a, previously reported data are also shown for comparison (Kramer et al., 2001). Note that our data generally are in good agreement with those previous data. Fig. 1b shows that the BSF depends on the irradiated area of the phantom, reaching saturation at large irradiated area

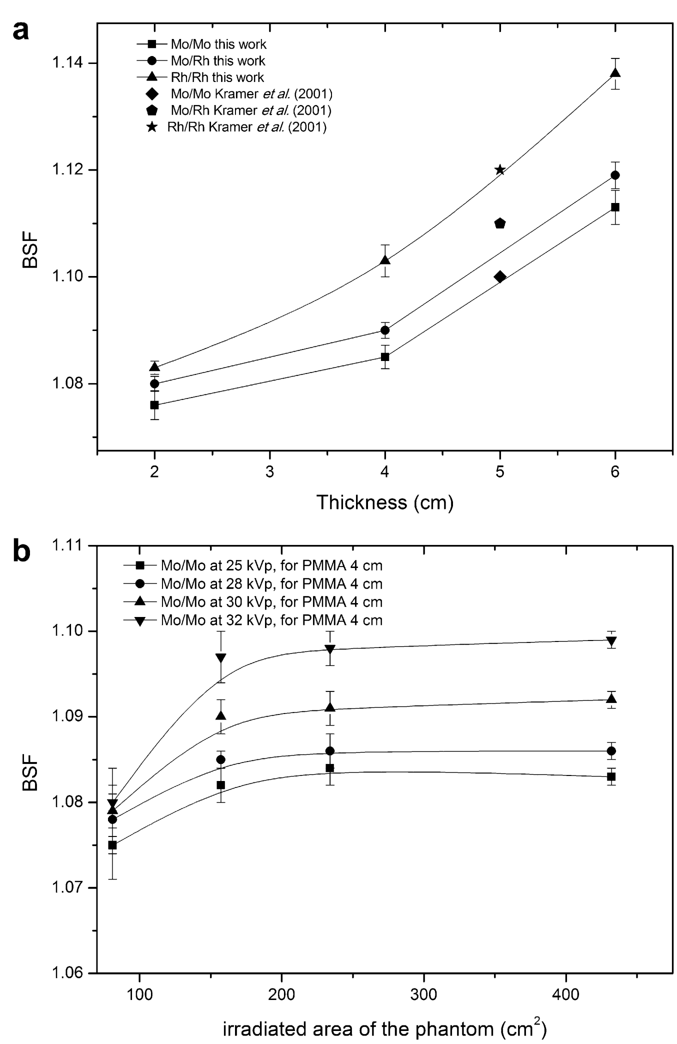

Fig. 1. Dependence of backscatter factors on (a) the phantom thickness for different anode-filter combinations at 28 kVp together obtained data from Kramer et al. (2001) (b) Values BFS for different irradiated areas of the phantom and tube voltages for Mo/Mo combination.

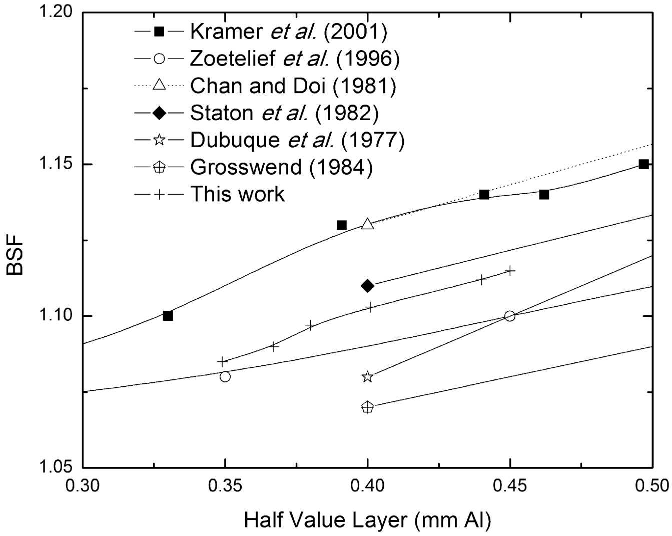

Fig. 2. Comparison of the BSF for different beam qualities (HVL mm of Al), for PMMA phantom of 4 cm, together the available published data.

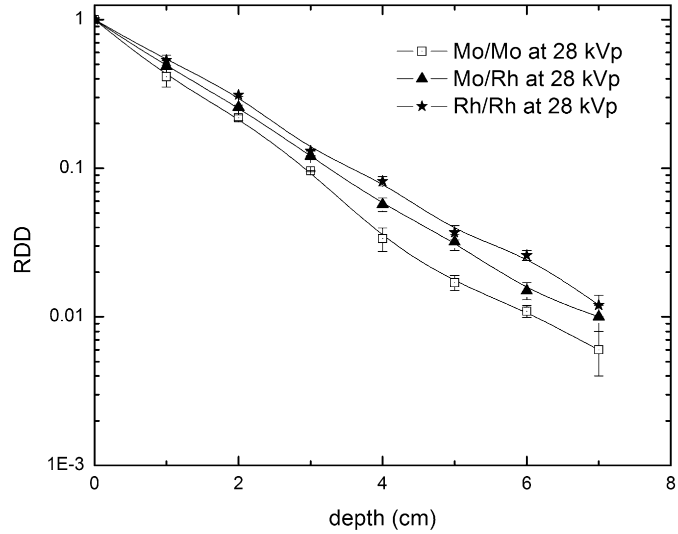

Fig. 4. Relative Dose at different depths for different anode-filter combinations at 28 kVp.

(around 200 cm^2). The results obtained about the effect of focus-image detector distance on the BFS showed that this parameter does not influence the BSF significantly in the range considered for this work.

Fig. 2 shows the results obtained for the values of BSF for different beam qualities, expressed in terms of the half-value layer (HVL) of aluminum, for PMMA phantom of 4 cm, together the available published data (Dubuque et al., 1977; Chan and Doi, 1981; Stanton et al., 1981; Grosswendt, 1984; Zoetelief et al., 1996; Kramer et al., 2001). As can be observed in the figure, the BSF increases with increasing values of the HVL Al, this behavior is related to the increase of the amount of scattering with increasing beam quality (energy). The existing differences between the absolute values obtained in this work and those presented in literature can be attributed to differences in beam spectra and the experimental techniques used as well as differences in the geometric model adopted in Monte Carlo calculations. The dependence with the tube voltages shows a slight positive trend (about 0.5% per kVp).

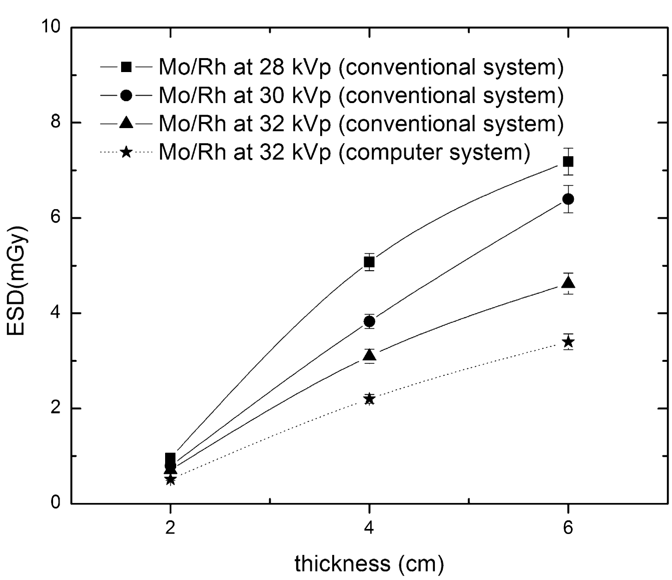

Fig. 3. ESD as a function of PMMA phantom thickness at different tube potentials. Solid curves are results for the conventional system and the dot curve for the computer system (at 32 kVp).

The values and trends of BSF obtained for computer mammography equipment are very similar, despite possible differences in beam energy spectra.

Fig. 3 shows the ESD as a function of the PMMA phantom thickness at different tube voltages. As expected the ESD values increase with increasing phantom thicknesses and decrease with increasing tube voltage (or effective energy of the beam). The results also indicate that ESD values are lower (around 40%) for computer mammography.

Relative dose as a function of depth for different anode-filter combinations at 28 kVp, for a 7 cm PMMA thickness are shown in Fig. 4. These curves decrease nearly exponentially with the depth, being more pronounced for Mo/Mo and less for Rh/Rh. This trend was expected and it is related to the fact that beams with high effective energies (high beam qualities) are less attenuated. The observed trends are in good agreement with those reported in literature (Hammerstein et al., 1979; Stanton et al., 1984). Nevertheless, the differences, in absolute values, are mainly due to phantom composition used in the previous measurements.

4. Conclusions

The experimental technique used in this work is simple, fast and allows investigating the dependency of BFS, ESD and RDD with the HVL, tube voltage, anode-filter combination, irradiated area and thickness of the phantom with uncertainties between 2 and 5%.

Our experimental values obtained with the TLD-100 are in satisfactory agreement with previously published values. From our experimental data for PMMA phantom can be observed that the BFS values show a slight dependence on phantom thickness, HVL and anode-filter combination, and less slight dependence on tube voltage. Concerning to the dependence the BSF values with the distance focus-film and irradiated area, our results show that the former does not have influence on the BSF values, while the latter raises the BFS values up to reaching saturation values at very large area (up to 200 cm^2). ESD values showed a strong dependence on the various parameters considered, especially with the phantom thickness. RDD curves were investigated experimentally showing dependence nearly exponential and strongly dependent on the spectral conditions.

Acknowledgments

This work was supported by the Brazilian agencies Conselho Nacional de Desenvolvimento Científico e Tecnológico (CNPq) and Fundação de Amparo à Pesquisa do Estado de São Paulo (FAPESP).

References

Aznar, M.C., Hemdal, B., Medin, J., Marckmann, C.J., Andersen, C.E., Bøtter-Jensen, L., Andersson, I., Mattsson, S., 2005. In vivo absorbed dose measurements in mammography using a new real-time luminescence technique. Br. J. Radiol. 78, 328–334.

Carlsson, C.A., 1993. Differences in reported backscatter factors for low-energy X-rays: a literature study. Phys. Med. Biol. 38, 521–531.

Carlsson, G.A., Dance, D.R., 1992. Breast absorbed doses in mammography: evaluation of experimental and theoretical approaches. Radiat. Prot. Dosim. 43, 197–200.

Chan, H.P., Doi, K., 1981. Monte carlo simulation studies of backscatter factors in mammography. Radiology 139, 195–199.

Cunha, D.M., Tomal, A., Poletti, M.E., 2010. Evaluation of scatter-to-primary ratio, grid performance and normalized average glandular dose in mammography by Monte carlo simulation including interference and energy broadening effects. Phys. Med. Biol. 55, 4335–4359.

Dance, D.R., 1990. Monte carlo calculation of conversion factors for the estimation of mean glandular breast dose. Phys. Med. Biol. 35, 1211–1219.

Dance, D.R., Skinner, C.L., Carlsson, G.A., 1999. Breast dosimetry. Appl. Radiat. Isot. 50, 185–203.

Dubuque, G.L., Cacak, R.K., Hendee, W.R., 1977. Backscatter factors in the mammographic energy range. Med. Phys. 4, 397–399.

Grosswendt, B., 1984. Backscatter factors for X-rays generated at voltages between 10 and 100 kV. Phys. Med. Biol. 29, 579–591.

Grosswendt, B., 1990. Dependence of the photon backscatter factor for water on source-to-phantom distance and irradiation field size. Phys. Med. Biol. 35, 1233–1245.

Hammerstein, G.R., Miller, D.W., White, D.R., Masterson, M.E., Woodard, H.Q., Laughlin, J.S., 1979. Absorbed radiation dose in mammography. Radiology 130, 485–491.

Harrison, R.M., Walker, C., Aukett, R.J., 1990. Measurement of backscatter factors for low energy radiotherapy (0.1–2.0 mm Al HVL) using thermoluminescence dosimetry. Phys. Med. Biol. 35, 1247–1254.

Klevenhagen, S.C., 1989. Experimentally determined backscatter factors for X-rays generated at voltages between 16 and 140 kV. Phys. Med. Biol. 34, 1871–1882.

Kramer, R., Drexler, G., Petoussi-Henss, N., Zankl, M., Regulla, D., Panzer, W., 2001. Backscatter factors for mammography calculated with Monte carlo methods. Phys. Med. Biol. 46, 771–781.

Stanton, L., Brattelli, S.D., Day, J.L., Stanton, R.E., Villafana, T., 1982. Measurements of diagnostic X-ray backscatter by a novel ion chamber method. Med. Phys. 9, 121–130.

Stanton, L., Day, J.L., Brattelli, S.D., Lightffot, D.A., Vince, M.A., Stanton, R.E., 1981. Comparison of ion chamber and TLD dosimetry in mammography. Med. Phys. 8, 792–798.

Stanton, L., Villafana, T., Day, J.L., Lightffot, D.A., 1984. Dosage evaluation in mammography. Radiology 150, 577–584.

Tomal, A., Cunha, D.M., Poletti, M.E., 2010. Establishment of the mammographic radiation qualities in industrial equipment: spectra determination. Nucl. Instrum. Methods Phys. Res. Sect. A, Accel. Spectrom. Detect. Assoc. Equip.. doi:10.1016/j.nima.2010.08.055.

Zoetelief, J., Fitzgerald, M., Leitz, W., Säbel, M., 1996. European Protocol on Dosimetry in Mammography. European Commission Report 16263 EN (Luxembourg: European Comission).